Journal of Marine Science and Technology

Volume 22 | Issue 6 Article 13

MODELING AND CONTROL OF A NOVEL BALL SCREW MECHANISM

Wen-Hsiang Hsieh
Department of Automation Engineering, National Formosa University, Huwei, Yunlin, Taiwan, R.O.C., allen@nfu.edu.tw

Kai-Bi Chang
Department of Automation Engineering, National Formosa University, Huwei, Yunlin, Taiwan, R.O.C.

MODELING AND CONTROL OF A NOVEL BALL SCREW MECHANISM

Acknowledgements

The supports of the National Science Council, Republic of China (Taiwan), under Grants NSC 101-2221-E-150-037 and NSC 98-2622-E-150-064-CC3 are gratefully acknowledged.

Journal of Marine Science and Technology, Vol. 22, No. 6, pp. 754-761 (2014)
DOI: 10.6119/JMST-014-1028-2

MODELING AND CONTROL OF A NOVEL BALL SCREW MECHANISM

Wen-Hsiang Hsieh and Kai-Bi Chang

Key words: ball screw, Oldham coupling, refined PID control.

ABSTRACT

This study proposes a systematic approach for the design and control of a novel ball screw transmission system. We investigated the structure of the system, performed kinematic analysis, and conducted dimensional synthesis by optimization. The mathematical model of the system was determined by system identification and a refined PID controller was designed. Computer simulation was conducted to verify the feasibility of the proposed design. A prototype machine and an experimental setup were built and tested. The experimental results show that the output with the controller agrees well with the required output. Therefore, the proposed design can produce the expected output with high accuracy.

I. INTRODUCTION

A ball screw is a mechanism that converts motion between rotation and rectilinear motion by direct contact. It comprises many balls that circulate between the cap and screw, as shown in Fig. 1. In general, the screw is the driver, and the cap is the driven. A ball screw has many advantages, e.g., high precision, long service life, and low friction, and is widely used in various machinery.

The motion requirement in some machines is to convert rectilinear motion into rotatory motion, i.e., the cap is the driver to produce rectilinear motion and drive the screw to rotate. Despite its wide application in many kinds of machines, very few rigorous studies on this topic have been made.

Many investigations have been made of the use of variable speed or servo motors to improve kinematic performance of a mechanism or to generate complex motion. Rothbart [21] presented a cam mechanism driven by a quick return mechanism at non-uniform speed. Tesar and Matthew [23] derived the equations for the follower motion in a case where the cam is driven by variable input. Hsieh [4] was first to present a novel approach to improve the state of the motion of the follower by varying the input speed using a servomotor. Later, Yan *et al*. [24-27] contributed to improve the output motion of a mechanism using a servomotor solution. Liu *et al*. [14] reduced the peak acceleration of a ball screw by driving with a servo driven crank-slider mechanism. Mundo and Yan [17] optimized the kinematics of a ball-screw transmission mechanism using non-circular gears for mechanical control of the output motion. Hsieh [3, 5-8] commenced a series of investigations on cam-controlled planetary gear trains (CCPGTs), including kinematic and experimental studies [3], structural synthesis [8], kinematic synthesis [5], and kinetostatic and mechanical efficiency Studies [6, 7].

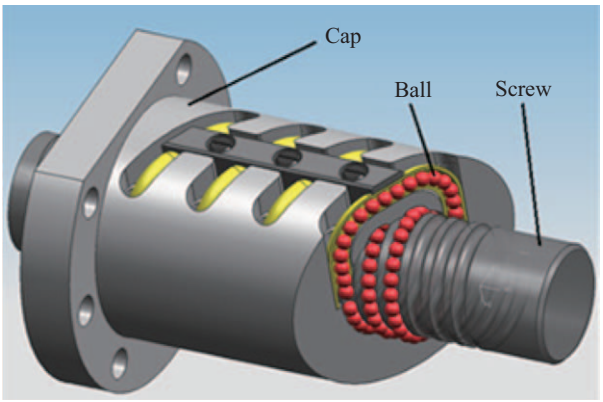

Fig. 1. Ball screw.

This study proposes a systematic approach for the design and control of a novel ball screw transmission system. Section 2 introduces the composition of the novel system. Section 3 presents an optimization approach for dimensional synthesis. Section 4 addresses the design approach of a refined PID controller. In Section 5, an illustrative example is given. Some final conclusions are summarized in Section 6.

II. KINEMATIC ANALYSIS

The proposed system consists of a motor, a reduction gear, a variable speed coupling, a slider-crank mechanism, and a ball screw, as shown in Fig. 2. The motor with a gear reducer installed is connected to the slider-crank mechanism by a

Paper submitted 05/06/14; revised 08/15/14; accepted 10/28/14. Author for correspondence: Wen-Hsiang Hsieh (e-mail: allen@nfu.edu.tw).
Department of Automation Engineering, National Formosa University, Huwei, Yunlin, Taiwan, R.O.C.

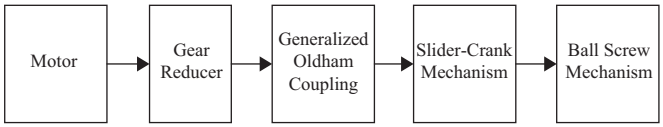

Fig. 2. Proposed ball screw system.

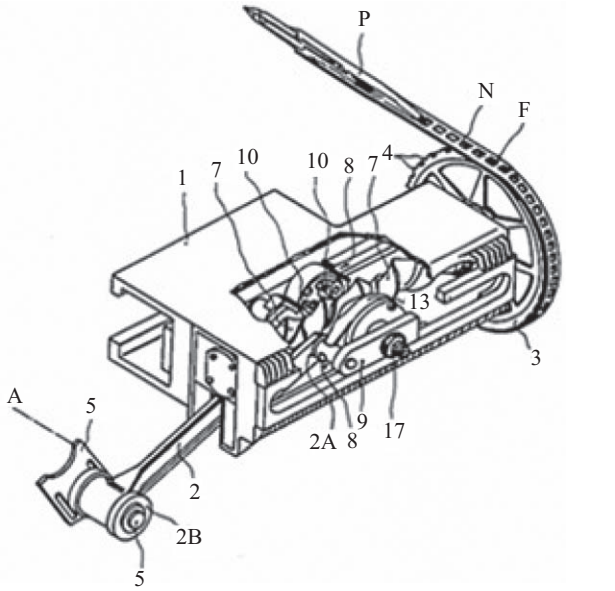

Fig. 3. Mechanism for weft insertion in a shuttle weaving loom [15].

generalized Oldham coupling, and the ball screw finally produces complex rotational output. Since the variable speed coupling in the proposed system can easily be replaced with various sizes of couplings, the configuration and assembly can also be changed. The position and speed of the output can be adjusted to meet various motion requirements. The stroke of the system can be adjusted by altering the length of the crank link and the offset of the ram; therefore, the output motion of the proposed system can be arbitrarily changed to meet various motion requirements. Compared to a ball screw driven by a servo motor, the proposed system is more cost effective and can transmit larger power. However, the adjustability of output motion is not as good as in the former arrangement. Potential applications are for machines that need various output rotation for each turn. For example, a mechanism that controls the motion of the weft insertion member in a shuttle weaving loom [19], as shown in Fig. 3.

Fig. 4 shows is a kinematic sketch of the proposed system. Points a_0 and b_0 denote the axes of rotation of the input and output disks. Points a and b denote the arc centers of the slots of the input and output disks. Point o is the point of intersection of the two arcs; oa = r_1 and ob = r_2 are the radii of the circular slots of input disk and output disk; e is the offset between the center c of the slider and the centerline a_0b_0. Angle $\alpha = \angle a_o b$ defines the intersection angle between two circular arcs; b_0b and bc are the link lengths of the crank and the connecting rod. Angle $\gamma = \angle a_0b_0b$ represents the relative position

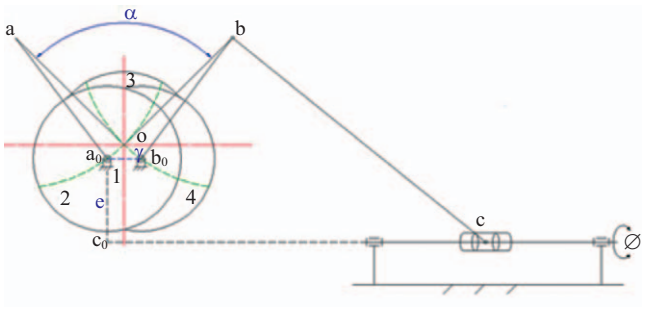

Fig. 4. Structural sketch.

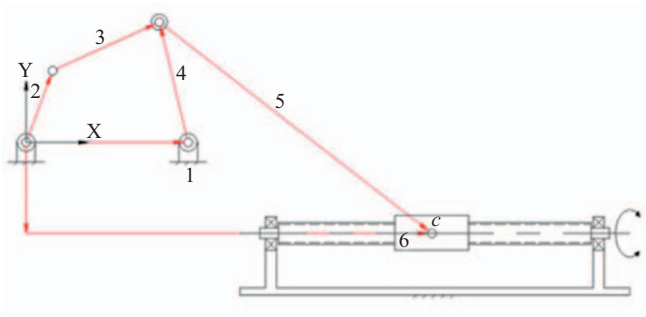

Fig. 5. Equivalent linkage.

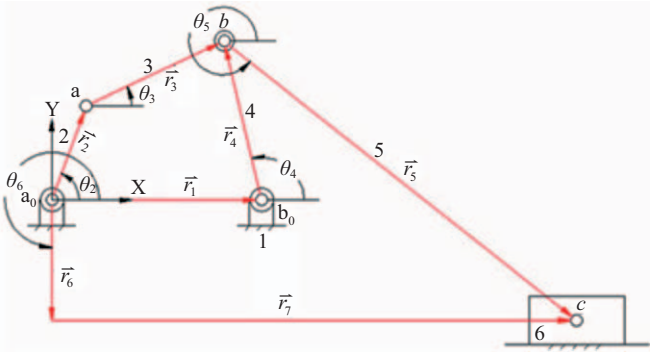

Fig. 6. Vector representation.

of the assembly between the coupling and the slider-crank mechanism, and the output motion will vary with different γ. The kinematic dimensions of the system can be fully defined if r_1, r_2, α, γ, a_0b_0, a_0a, b_0b, bc, and e are specified.

1. Position Analysis

A generalized coupling can be converted into a kinematically equivalent four-bar linkage [2, 10]. To perform kinematic analysis, the proposed mechanism is transformed into its equivalent linkage, as shown in Fig. 5. For simplification, the line connecting a_0 and b_0 is assumed to be parallel with the motion of the nut. Apparently, the mechanism is a planar linkage with 6 links and 7 joints. Kinematic analysis is conducted using the vector loop approach, and each vector is labeled as shown in Fig. 6, where the ball screw is not considered in the analysis.

$$\vec{r}_2 + \vec{r}_3 - \vec{r}_1 - \vec{r}_4 = 0 \quad (1)$$

$$\vec{r}_1 + \vec{r}_4 + \vec{r}_5 - \vec{r}_6 - \vec{r}_7 = 0 \quad (2)$$

where $\vec{r}_i$ (i = 1-7) is the vector of each kinematic dimension. Solving Eqs. (1) and (2) simultaneously, the position of each link can be obtained. The detailed procedure for solving position, velocity, and acceleration can be found in Ref. [18], and will not be repeated here. The angular displacement of the ball screw ϕ can be expressed as

$$\phi = \frac{2\pi}{p} r_7 \quad (3)$$

where p is the pitch of the screw.

III. OPTIMUM DESIGN

Optimization is the process of finding the conditions that give the maximum or minimum value of a function [20]. More specifically, optimization is an iterative process or method for finding the appropriate values of the parameters for a given problem by maximizing or minimizing the objective function subject to the given constraints. Traditionally, dimensional synthesis is performed by the accuracy point approach; however the available number of accuracy points is limited by the number of kinematic dimensions. Also, when the number of links is more than six, it is difficult to perform dimensional synthesis using the approach. Most practical optimization approaches are, in essence, numerical techniques, and the numbers of accuracy points and links are not limited. Therefore, this study employed the optimization method for dimensional synthesis.

To generate the desired output motion with precision, the error between the actual and the specified rotational speeds has to be minimized. Therefore, the objective function and design constraints are set as:

$$\min. \quad f(r_1, r_2, r_3, r_4, r_5, r_6, r_7) = \sum_{i=1}^{n} (\dot{\phi}_i - \dot{\phi}_{si})^2 \quad (4)$$

$$s.t. \quad g_j = l_j \le r_j \le u_j \quad (5)$$

where r_j (j = 1~7) are the kinematic dimensions of the ball screw system, $\dot{\phi}_{si}$ (i = 1~n) is the specified rotational speed of the screw, n is the number of the specified accuracy points, and $\dot{\phi}_i$ (i = 1~n) is the rotational speed of the screw, obtained from the kinematic analysis of the Eq. (3), and l_j and u_j are the lower and upper limits.

IV. CONTROLLER DESIGN

A motion control is required for the proposed system to produce precise output motion. Therefore, a controller design has to be conducted.

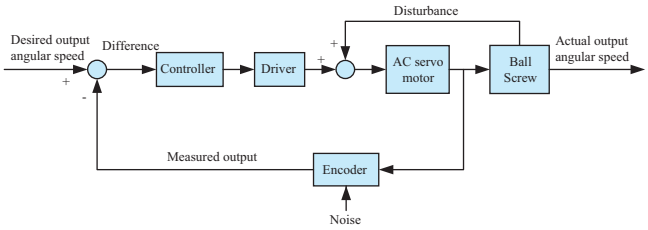

Fig. 7. Semi-closed-loop control system.

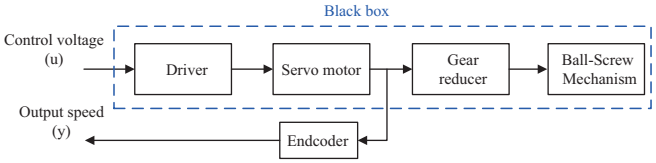

Fig. 8. System identification architecture.

1. Control Loop

Fig. 7 shows the block diagram of semi-closed-loop control for the proposed system. Firstly, the input is the desired output angular speed, and the difference between it and the speed of the AC servo motor measured by an encoder is forward to the implemented controller. Next, the servo driver converts the output command of the driver into the required voltage for driving the servo motor. Finally, the ball screw is driven by the servo motor to generate the output angular speed.

2. System Identification

System modeling deals with the problem of building the mathematical models of dynamic systems based on the observed data from the systems [16]. It is an iterative process and the initial step in the model-based control design. To design the controller, the mathematical model of the system (i.e., the servo motor and the ball screw) has to be formulated firstly. The mathematical model of the system can be found by principles of physics or system identification techniques. Since the proposed system is complicated and highly nonlinear, its mathematical model is difficult to be derived. Therefore, the system identification technique is used to establish the transfer function of the proposed system. The driver and the servo motor, where the reduction gear and the proposed ball screw mechanism are considered as its loading, are set as a black box for system identification. The input of the black box is the output voltage from the controller, and the measured data are the rotational speed of the servo motor as shown in Fig. 8.

The approach employed in system identification can be classified as a parametric or non-parametric model [9, 15, 18]. For a parametric model, the structure is chosen and the parameters are estimated for best fit. For a non-parametric model the structure is not chosen previously but determined from data. Parametric models are suitable for controller design

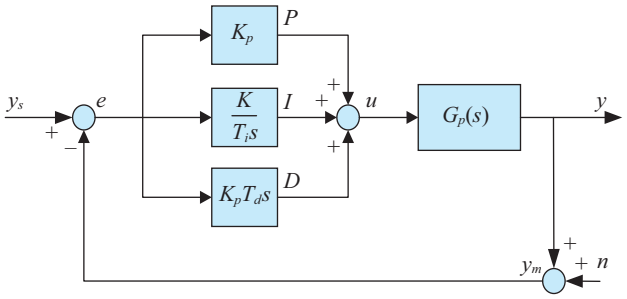

Fig. 9. PID control system.

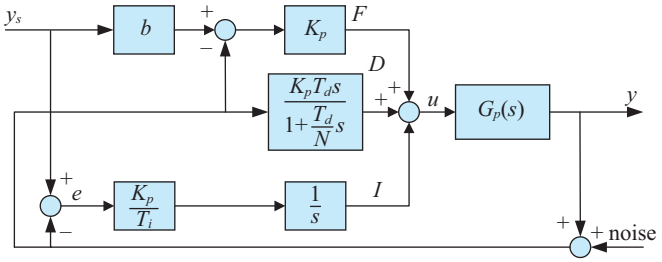

Fig. 10. Refined PID Control.

and simulation, hence are used in this study. A parametric model can be represented by a transfer function or state space model. For complicated systems, e.g., high order or with multiple inputs and outputs, state space models are appropriate representations. For a simple system, transfer functions model can be employed. In addition, the proposed system is non-linear and time-variant, it has been approximated as a linear and time-invariant system to simplify the complexity in design and analysis.

3. Refined PID Control

A PID controller is usually implanted as follows:

$$u(t) = K_p \left[e(t) + \frac{1}{T_i}\int_0^t e(\tau)d\tau + T_d \frac{de(t)}{dt} \right] \tag{6}$$

where u is the controller output; K_p, T_i, and T_d are the proportional gain, the integration time, the derivative time; and $e(t)$ is the error between the set-point $y_s(t)$ and the measured output $y_m(t)$:

$$e(t) = y_s(t) - y_m(t) \tag{7}$$

$y_m(t)$ equals the system output $y(t)$ subtracted by the measured noise $n(t)$:

$$y_m(t) = y(t) - n(t) \tag{8}$$

Taking the Laplace transform with respect to Eq. (6), the transfer function of the controller $G_c(s)$ can then be expressed as:

$$G_c(s) = \frac{u(s)}{e(s)} = K_p\left(1 + \frac{1}{T_i s} + T_d s\right) \tag{9}$$

Fig. 9 shows the block diagram of a closed-loop system with a PID controller.

A refined PID controller was proposed by Astrom & Hagglund [24], and it can be expressed as:

$$u(t) = K_p \left\{ [by_s(t) - y_m(t)] + \frac{1}{T_i}\int_0^t e(\tau)d\tau \right\} + D(t) \tag{10}$$

where a set-point weighting factor b multiplied by $y_s(t)$ is added, it is normally in the range of $0 < b < 1$. Moreover, the derivative part is modified from

$$D(t) = K_p T_d \frac{de(t)}{dt} = K_p T_d \left[\frac{dy_s(t)}{dt} - \frac{dy_m(t)}{dt}\right] \tag{11}$$

to

$$D(t) = -\frac{T_d}{N}\frac{dD(t)}{dt} - K_p T_d \frac{dy_m(t)}{dt} \tag{12}$$

where N is the noise filtering constant, and usually ranges between 3 and 10. The weighting factor adds flexibility for adjustment of the response between $u(t)$ and $y_s(t)$. And the modification of $D(t)$ can limit the amplification of high-frequency measurement noise by a factor of $K_p N$ at most. The above advantages made the refined PID controller suitable for use in this study. Taking Laplace transform with respect to Eq. (12), yields:

$$D(s) = -\frac{K_p T_d s}{1 + \frac{T_d}{N}s} y_m(s) \tag{13}$$

The block diagram, shown in Fig. 9, of the closed-loop system with a refined PID controller, can be modified as shown in Fig. 10.

4. Tuning of the Refined PID Parameters

Tuning of the PID controller is an optimization problem to find a set of parameters that best fit the requirements. In the early stages, the controller is tuned by the intuitive experience of the designer. The Ziegler-Nichols method [28] is the first approach for tuning PID controllers, it can produce a feasible design, but not an optimal one. After this, the genetic algorithm based PID tuning approach [12, 13] is presented. Since a tuning approach based on the genetic algorithm can reach an optimum solution, it will be used here for tuning the refined PID control parameters. The objective function and the constraints are specified as:

$$Min.\ e_{ss}(b, K_p, T_i, T_d) = \sum_{k=0}^{n} \left[y(k) - y_s(k) \right]^2 \tag{14}$$

$$\begin{aligned} s.t.\ & 0 < K_p < K_u \\ & 0 < T_i < T_u \\ & 0 < T_d < T_u \\ & 0 < b < 1 \end{aligned} \tag{15}$$

where the objective function e_{ss} is set as the sum of the square error $y(k)$, and b, K_p, T_i, and T_d are the design variables. In addition, K_u and T_u are the ultimate gain and the ultimate period of the process [22].

The aim of an optimization problem is to minimize its cost function. However, the offspring in GA is generated with the individual that has the highest fitness function value. Therefore, the fitness function $F(b, K_p, T_i, T_d)$ can be set as the inverse of the objective function:

$$F(b, K_p, T_i, T_d) = \frac{1}{e_{ss}(b, K_p, T_i, T_d)} \tag{16}$$

where $F(b, K_p, T_i, T_d) = 0$, if any of the following conditions holds

(1) The system with b, K_p, T_i, and T_d is unstable.
(2) Any one of b, K_p, T_i, and T_d is negative.
(3) $M_s > m_s$.

where m_s is the specified low bound, and M_s is the inverse of the shortest distance from the Nyquist curve of the loop transfer function $G_l(j\omega)$ to the critical point -1, and is defined as

$$M_s = \max_{\omega} \left| \frac{1}{1 + G_l(j\omega)} \right| \tag{17}$$

which is a measure of the stability robustness. Having established the fitness function, GA can be applied to find the parameters of the PID controller.

V. DESIGN EXAMPLE

To illustrate the proposed approach, a design example is given here, and the feasibility is verified by computer simulation.

1. Optimization

Fig. 11 shows the nine specified angular speeds ϕ_{si} (i = 1-9), and the objectice function can be obtained by substituting the above speeds into Eq. (4). Moreover, the design constraints are set, based on the consideration of the space, as

Table 1. Optimized kinematic dimensions.

Kinematic dimensions	r_1	r_2	r_3	r_4	r_5	r_6
Value	13.29	60.00	84.85	60.00	175.00	50.00

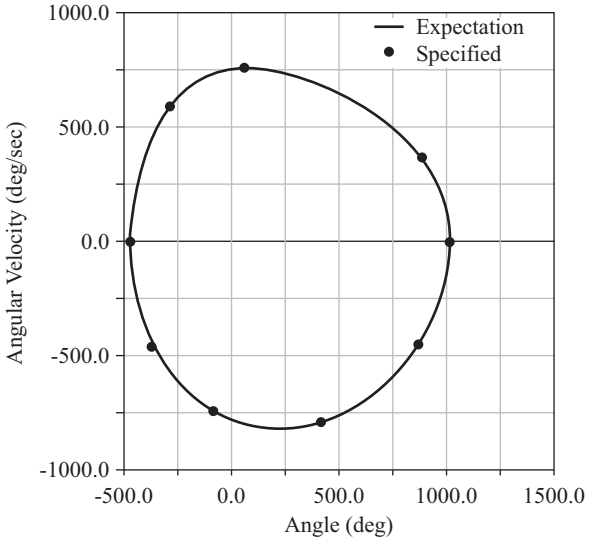

Fig. 11. Specified output angular velocity.

$$\begin{aligned} s.t.\quad & g_1 = 5 \le r_1 \le 30 \\ & g_2 = 50 \le r_2 \le 60 \\ & g_3 = 85 \le r_3 \le 100 \\ & g_4 = 60 \le r_4 \le 70 \\ & g_5 = 175 \le r_5 \le 200 \\ & g_6 = 20 \le r_6 \le 50 \end{aligned} \tag{18}$$

Since the objective function and the design constraints have been obtained, the optimization problem is formulated. It is a constrained nonlinear optimization problem, and can be solved by employing the **fmincon** function (SQP based, with the medium scale option) in the optimization toolbox of MATLAB software. The optimized dimensions are found and shown in Table 1.

2. Controller Design

The system model is established by the system identification technique, and the transfer function of the parametric model is used in this study. The system identification toolbox in the MATLAB is employed and revealed that the second order system model is a better fit than those of the first and third orders. The model can be expressed as

$$G(s) = \frac{V_{out}(s)}{V_{in}(s)} = \frac{1778}{s^2 + 81.15s + 1813} e^{-0.0188s} \left(\frac{V}{V}\right) \tag{19}$$

Fig. 12 depicts its Bode plot. It shows that the identified

Table 2. GA parameters.

Generation	200
Population	100
Crossover rate	40%
Mutation rate	1%
Sensitivity	2.0

Table 3. Refined PID parameters.

K_p	T_i	T_d	b
1.5396	0.5203	0.01808	1.6685

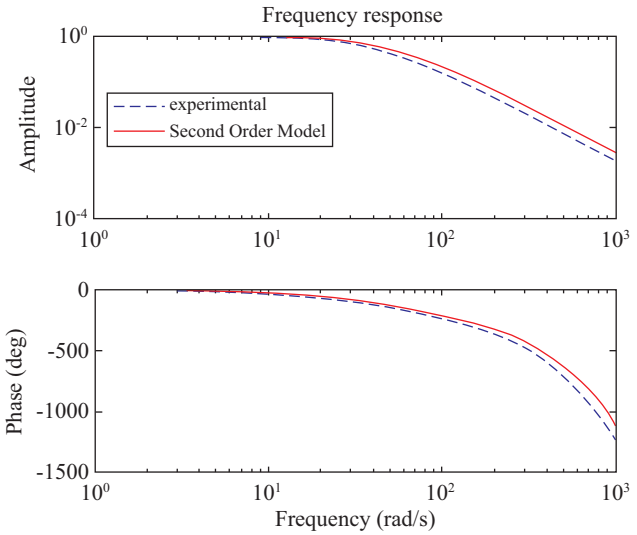

Fig. 12. Bode plot.

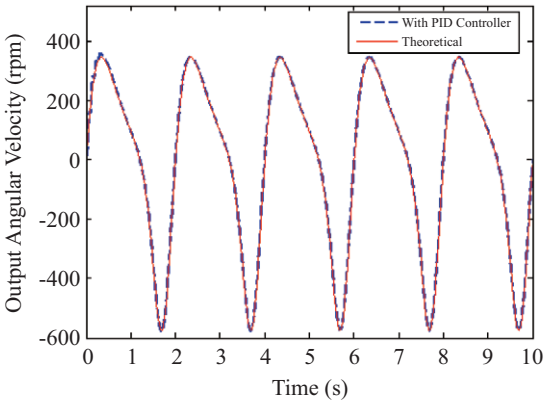

Fig. 13. Output speed (simulation).

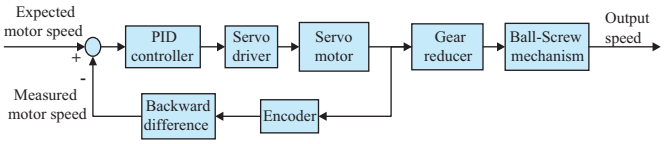

Fig. 14. Schematic of the experiment setup.

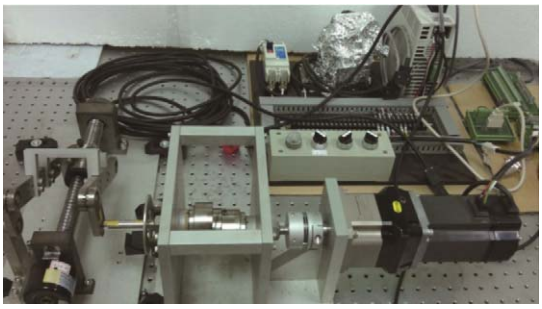

Fig. 15. Experimental setup.

model almost coincides with the experimental one at low frequency (< 300 Hz), and also have an adequate agreement at high frequency. The model described by Eq. (19) is a good representation of the proposed system.

The refined PID controller is implemented in the proposed system. Table 2 shows the specified parameters of GA, and Table 3 depicts the refined PID parameters obtained by GA.

3. Simulation

The feasibility of the controller design is verified by Simulink software, and the comparison between the output speeds is shown in Fig. 13. It is found that the speed with the proposed controller (dashed) agrees well with the theoretical (solid). Evidently, the controller can theoretically improve the performance of the system.

VI. EXPERIMENT

To verify the effectiveness of the proposed design, a test rig with a prototype is built as shown in Figs. 14 and 15. The system consists of a motion control card (Sensoray, Model 626), a servo motor (Mitsubishi, HC-KFS73) with a servo driver (MR-J2S-70A), a gear reducer (Apex Dynamics, AB090-010-S2-P1), the proposed ball-screw mechanism, and an encoder (Hontko, HTR-HM-12-900-3-L-M322). The input command of the system is the expected motor speed, and its difference from the measured motor speed is the input of the controller (installed in Model 626). The controller drives the servo motor using the servo driver, and the ball-screw mechanism rotates, driven by the motor through the gear reducer.

The comparisons of the experimental output speeds are shown in Fig. 16. The sums of the square errors between the experimental output speeds (with and without the PID controller) and the theoretical are 271987 rpm^2 and 3575404 rpm^2, respectively, hence the reduction of the errors is 92%. Apparently, the proposed controller can effectively enhance the accuracy of the output motion.

VII. CONCLUSIONS

In this work, a systematic approach for the modeling, design, and control of a novel ball screw transmission system has

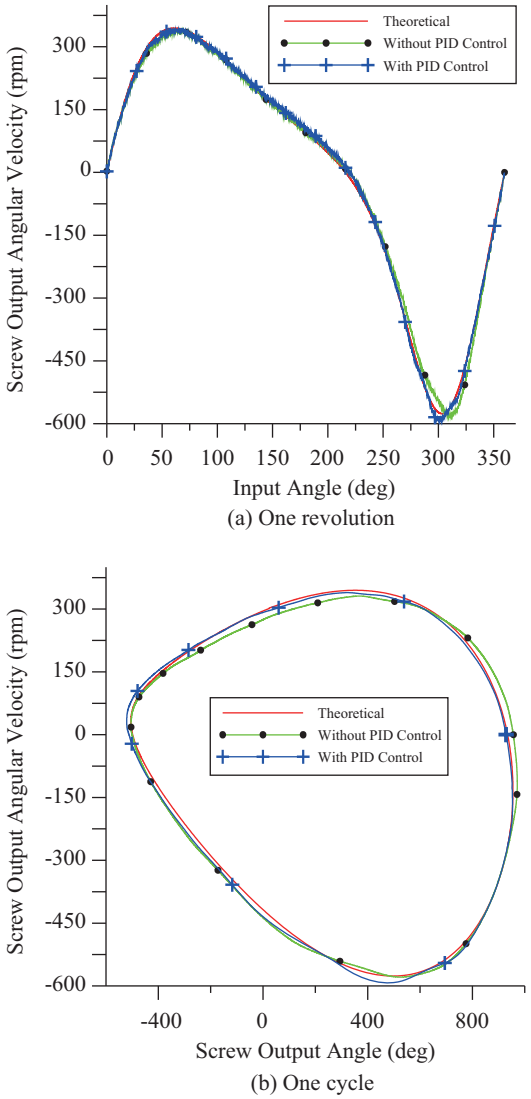

Fig. 16. Comparisons of output speeds.

been proposed. The structure of the proposed design has been addressed, and kinematic analysis has been conducted. The kinematic optimization has been performed. The refined PID control has been implemented. Simulated and experimental studies have been conducted. The results show that the proposed system can generate the expected motion, and its motion accuracy can be enhanced by the proposed approach.

ACKNOWLEDGMENT

The supports of the National Science Council, Republic of China (Taiwan), under Grants NSC 101-2221-E-150-037 and NSC 98-2622-E-150-064-CC3 are gratefully acknowledged.

REFERENCES

1. Astrom, K. J. and Hagglund, T., *PID Controllers: Theory, Design and Tuning*, Instrument Society of America, Research Triangle Park, NC (1995).
2. Freudenstein, F., Tsai, L. W., and Maki, E. R., "Generalized Oldham coupling," *Journal of Mechanisms, Transmissions, and Automation in Design*, Vol. 106, No. 4, pp. 475-481 (1984).
3. Hsieh, W. H., "An experimental study on cam-controlled planetary gear trains," *Mechanism and Machine Theory*, Vol. 42, No. 5, pp. 513-525 (2007).
4. Hsieh, W. H., *Improving the State of Motion of Followers by Controlling Cam Speed*, Master Thesis, Graduate School of Mechanical Engineering, National Cheng-Kung University, Tainan, Taiwan (1991). (In Chinese)
5. Hsieh, W. H., "Kinematic synthesis of cam-controlled planetary gear trains," *Mechanism and Machine Theory*, Vol. 44, No. 5, pp. 873-895 (2009).
6. Hsieh, W. H., "Kinetostatic and mechanical efficiency studies on cam-controlled planetary gear trains-part I theoretical analysis," *Indian Journal of Engineering and Materials Sciences*, Vol. 20, No. 3, pp. 191-198 (2013).
7. Hsieh, W. H., "Kinetostatic and mechanical efficiency studies on cam-controlled planetary gear trains-part II design and experiment," *Indian Journal of Engineering and Materials Sciences*, Vol. 20, No. 3, pp. 199-204 (2013).
8. Hsieh, W. H. and Chen, S. J., "Innovative design of cam-controlled planetary gear trains," *International Journal of Engineering and Technology Innovation*, Vol. 1, No. 1, pp. 1-11 (2011).
9. Hsieh, W. H. and Lee, I. C., "Modelling and control of cam-controlled planetary gear trains," *International Journal of Modelling, Identification and Control*, Vol. 12, No. 3, pp. 272-279 (2011).
10. Hsieh, W. H. and Tsai, C. H., "A study on a novel quick return mechanism," *Transactions of the Canadian Society for Mechanical Engineering*, Vol. 33, No. 3, pp. 487-500 (2009).
11. Hsieh, W. H. and Tsai, C. H., "On a novel press system with six links for precision deep drawing," *Mechanism and Machine Theory*, Vol. 46, No. 2, pp. 239-252 (2011).
12. Jones, A. H. and De Moura Oliveira, P. B., "Genetic auto tuning of PID controllers, genetic algorithms in engineering systems: innovations and applications," *IEE Conference Publication*, No. 414, pp. 141-145 (1995).
13. Kristinsson, K., "System identification and control using genetic algorithms," *IEEE Transactions on Systems, Man, and Cybernetics*, Vol. 22, pp. 1033-1046 (1992).
14. Liu, J. Y., Hsu, M. H., and Chen, F. C., "On the design of rotating speed functions to improve the acceleration peak value of ball-screw transmission mechanism," *Mechanism and Machine Theory*, Vol. 36, No. 9, pp. 1035-1049 (2001).
15. Ljung, L., System Identification Toolbox: User's Guide, the Mathworks, Inc. (1998).
16. Ljung, L., *System Identification: Theory for the User*, 2nd ed., Prentice Hall, New Jersey (1999).
17. Mundo, D. and Yan, H. S., "Kinematic optimization of ball-screw transmission mechanism," *Mechanism and Machine Theory*, Vol. 42, No. 9, pp. 34-47 (2007).
18. National Instruments, *LabVIEW System Identification Toolkit User Manual*, Part No. 371001B-01, September (2004).
19. Pezzoli, L., "Mechanism to control the movements of weft insertion members in shuttleless weaving looms," *United States Patent*, No. 4624288 (1986).
20. Rao, S. S., *Engineering Optimization: Theory and Practice*, 4th Ed., John Wiley & Sons, Hoboken, N.J. (2009).
21. Rothbart, H. A., *Cams: Design, Dynamics and Accuracy*, Wiley, New York (1956).
22. Shen, J. C., "New tuning method for PID controller," *ISA Transactions*, Vol. 41, No. 4, pp. 473-484 (2002).
23. Tesar, D. and Matthew, G. K., *The Dynamic Synthesis, Analysis and Design of Modeled Cam Systems*, Lexington Books, Lexington, MA (1976).
24. Yan, H. S. and Fong, M. K., "An approach for reducing the peak acceleration of cam-follower systems using a b-spline representation," *Journal of the Chinese Society of Mechanical Engineers*, Vol. 15, No. 1, pp. 48-55 (1994).

25. Yan, H. S., Hsu, M. H., Fong, M. K., and Hsieh, W. H., "A kinematic approach for eliminating the discontinuity of motion characteristics of cam-follower systems," *Journal of Applied Mechanisms and Robotics*, Vol. 1, No. 2, pp. 1-6 (1994).
26. Yan, H. S., Tsai, M. C., and Hsu, M. H., "A variable-speed method for improving motion characteristics of cam-follower systems," *ASME Transactions, Journal of Mechanical Design*, Vol. 118, No. 1, pp. 250-258 (1996).
27. Yan, H. S., Tsai, M. C., and Hsu, M. H., "An experimental study of the effects of cam speed on cam-follower systems," *Mechanism and Machine Theory*, Vol. 31, No. 4, pp. 397-412 (1996).
28. Ziegler, J. B. and Nichols, N. B., "Optimum settings for automatic controllers," *ASME Transactions*, Vol. 64, pp. 759-768 (1942).